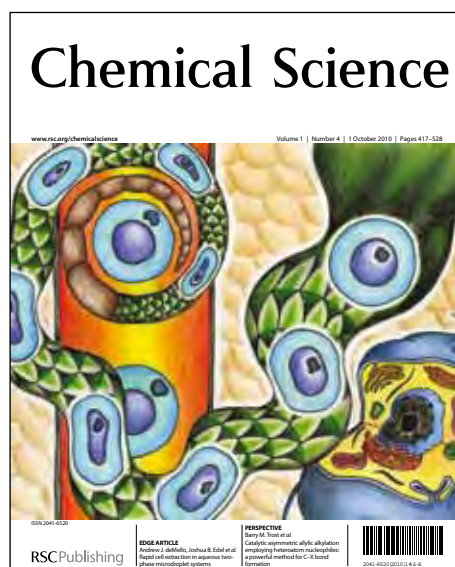


Chemical Science

Accepted Manuscript



This is an *Accepted Manuscript*, which has been through the RSC Publishing peer review process and has been accepted for publication.

Accepted Manuscripts are published online shortly after acceptance, which is prior to technical editing, formatting and proof reading. This free service from RSC Publishing allows authors to make their results available to the community, in citable form, before publication of the edited article. This *Accepted Manuscript* will be replaced by the edited and formatted *Advance Article* as soon as this is available.

To cite this manuscript please use its permanent Digital Object Identifier (DOI®), which is identical for all formats of publication.

More information about *Accepted Manuscripts* can be found in the [Information for Authors](#).

Please note that technical editing may introduce minor changes to the text and/or graphics contained in the manuscript submitted by the author(s) which may alter content, and that the standard [Terms & Conditions](#) and the [ethical guidelines](#) that apply to the journal are still applicable. In no event shall the RSC be held responsible for any errors or omissions in these *Accepted Manuscript* manuscripts or any consequences arising from the use of any information contained in them.

Sodium Phosphaethynolate, Na(OCP), as a “P” Transfer Reagent for the Synthesis of N-Heterocyclic Carbene Supported P₃ and PAsP Radicals

Aaron M. Tondreau,^a Zoltán Benkő,^a Jeffrey Harmer,^b Hansjörg Grützmacher^{a,c*}

^a Department of Chemistry and Applied Biosciences, ETH Zürich, CH-8093, Switzerland, hgruetzmacher@ethz.ch

^b Centre for Advanced Imaging, University of Queensland, St Lucia, QLD 4072, Australia, jeffrey.harmer@cai.uq.edu.au

^c Lehn Institute of Functional Materials (LIFM), Sun Yat-Sen University, 510275 Guangzhou, China.

Abstract

Sodium phosphaethynolate, Na(OCP), reacts as a P⁻ transfer reagent with the imidazolium salt [DippNHC-H][Cl] [DippNHC = 1,3-bis(2,6-diisopropylphenyl)imidazol-2-ylidene] to give the parent phosphinidene-carbene adduct, DippNHC=PH, with the loss of CO. In a less atom economic reaction, the cage compound, P₇(TMS)₃ (TMS = SiMe₃) reacts likewise with the imidazolium salt to yield DippNHC=PH thereby giving two entry points into parent phosphinidene based chemistry. From the building block DippNHC=PH, the carbene supported P₃ cation [(DippNHC)₂(μ-P₃)][Cl] was rationally synthesized using half an equivalent of PCl₃ in the presence of DABCO (1,4-diazabicyclo[2.2.2]octane). The corresponding arsenic analogue, [(DippNHC)₂(μ-PAsP)][Cl], was synthesized in the same manner using AsCl₃. The reduction of both [(DippNHC)₂(μ-P₃)][Cl] and [(DippNHC)₂(μ-PAsP)][Cl] into their corresponding neutral radical species was achieved simply by reducing the compounds with an excess of magnesium. This allowed the electronic structures of the compounds to be investigated using a combination of NMR and EPR spectroscopy, X-ray crystallography, and computational studies. The findings of the investigation into (DippNHC)₂(μ-P₃) and (DippNHC)₂(μ-PAsP) reveal the central pnictogen atom in both cases as the main carrier of the spin density (~60%), and that they are best

described as the P₃ or PAsP analogues of the elusive allyl radical dianion. The phosphorus radical was also able to undergo a cycloaddition with an activated acetylene, followed by an electron transfer to give the ion pair [(^{Dipp}NHC)₂(μ-P₃)] [P₃(C(COOMe))₂].

Introduction

Phosphorus atom transfer reagents continue to generate interest in main-group chemistry. Many phosphinidene (P–R) transfer reagents, like phosphanorbornadiene or (benzo)phosphepine complexes, utilize a transition metal carbonyl to stabilize the low coordinate phosphorus before adding a trapping compound.¹ These reagents have been used to transfer a phosphinidene fragment to a variety of substrates, which are predominantly unsaturated compounds like alkynes and alkenes. Phospha-Wittig reagents (R₃P=PR', formal adducts of a phosphane and a phosphinidene) also are able to transfer low coordinate phosphorus moieties to suitable substrates, however, their application is limited due to thermal instability.² Recently Cummins et al. reported a facile synthesis of uncomplexed dibenzo-7λ³-phosphanorbornadiene starting from magnesium anthracenide and selected phosphorus dichlorides.³ Upon thermolysis, anthracene is released and the phosphinidene fragment could be trapped with 1,3-cyclohexadiene. Detailed computational and preliminary synthetic efforts have also been undertaken to determine the suitability of phosphinidene complexes with annulated pyrazine and pyridine units as phosphinidene transfer reagents.⁴ A recent report by Driess et al. on the transfer of the parent phosphinidene from a silylene to an N-heterocyclic carbene presents a significant step forward in phosphorus transfer chemistry.⁵ This approach represents the state of the art but the synthesis of the silylene-phosphinidene adduct requires several steps. A disadvantage of the cited reactions is their inefficiency with respect to atom economy, often requiring metal complexes or generating

large amounts of side product. For these reasons the search for a more accessible phosphorus transfer reagent remains a challenge.

Synthetic phosphorus chemistry has historically treated P_7 derivatives [$P_7(\text{TMS})_3$, M_3P_7 ; $\text{TMS} = \text{SiMe}_3$; $M = \text{Li, Na, K}$] as end products and not as synthetically viable sources for single phosphorus atoms. The extent of chemistry revolving around the P_7 cage has been primarily limited to substitutions occurring at the nucleophilic P^- atoms. Recent works involving the destruction of the P_7 cage into P_5 and P_2 phosphorus fragments with $\text{Co}(\text{Mes})_2$ indicate that P_7 compounds can indeed be seen as a useful platform into phosphorus chemistry rather than a dead-end in synthesis.⁶ Goicoechea et al. reported the use of the protic P_7 cage to form 1,2,3-triphospholides with the use of alkynes.⁷ Furthermore, the carbonylation of K_3P_7 at 150 °C in DMF gives the potassium salt of the phosphoethynolate anion, $K(\text{OCP})$.⁸ The sodium salt, $\text{Na}(\text{OCP})$, can be accessed via a bond metathesis reaction between a niobium phosphido complex, $(L)_n\text{Nb}\equiv\text{P}$ and CO_2 .⁹ More conveniently, $\text{Na}(\text{OCP})$ can be prepared from the phosphide ion (PH_2^-) in a reaction with carbon monoxide or other CO sources (e.g. diethyl carbonate).¹⁰ The $(\text{OCP})^-$ anion can be regarded as an adduct of carbon monoxide and P^- and in this respect also offers the possibility of being a single phosphorus transfer reagent.

Much work has been devoted to exploring the stabilization of different main group element fragments with the use of N-heterocyclic carbenes (NHCs).¹¹ Main group fragments that would otherwise be too reactive, such as Si_2 ,¹² Ge_2 ,¹³ Sn_2 ,¹⁴ and B_2 ¹⁵ have been stabilized and isolated. Carbenes have also been used to activate P_4 to generate carbene-stabilized fragments of phosphorus, such as a P_2 and a linear P_4 bridging two carbenes.¹⁶ Robinson et al. achieved the synthesis of P_2 via the reduction of the carbene- PCl_3 adduct with KC_8 .¹⁷ This series has been extended to the P_3 cation in a fragmentation reaction with an NHC,¹⁸ but the neutral P_3 adduct

remains missing from the series. In order to fill the gap in this series, we aimed to synthesize the carbene stabilized catena P_3 and the related PAsP radicals, which, to the best of our knowledge, have not yet been reported. Because the spin delocalization in such radicals can be studied with EPR spectroscopy, detailed information on the electronic structure in such NHC stabilized main group element fragments can be gained.¹⁹

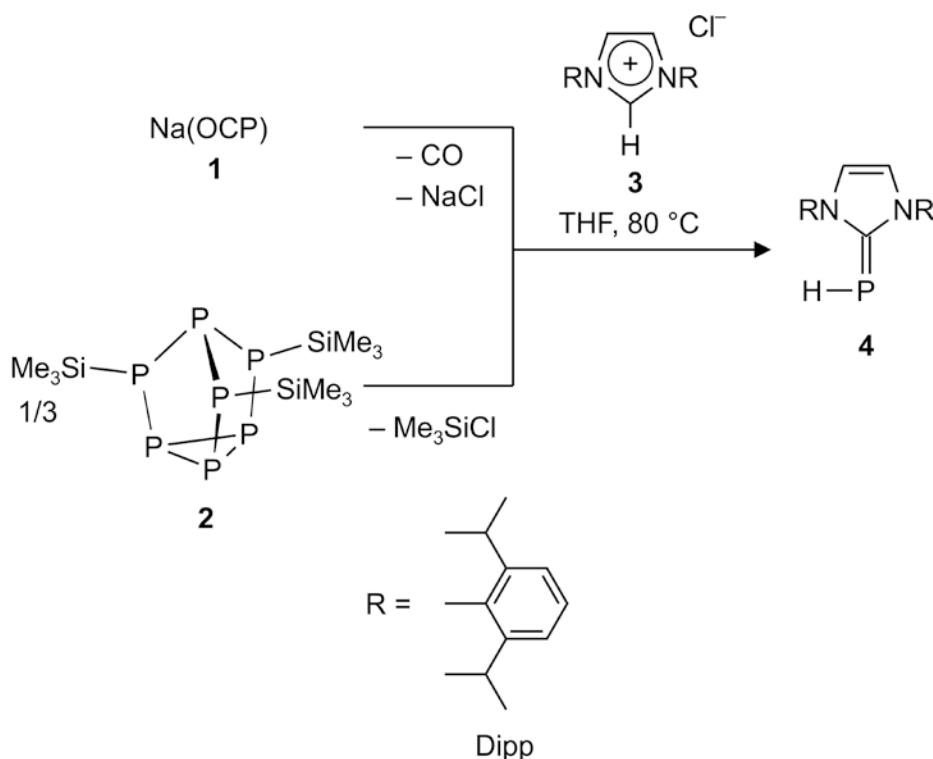
Herein we describe the synthesis of the organophosphorus complex $^{Dipp}NHC=PH$ utilizing $Na(OCP)$ as a P-atom donor. This transformation was also achieved with the cage compound $P_7(TMS)_3$ as the P-atom donor. Upon the addition of PCl_3 or $AsCl_3$ to $^{Dipp}NHC=PH$ in the presence of an amine base, $[(^{Dipp}NHC)_2(\mu-P_3)][Cl]$ or $[(^{Dipp}NHC)_2(\mu-PAsP)][Cl]$ were formed, respectively. Reduction to form the neutral radicals $(^{Dipp}NHC)_2(\mu-P_3)$ and $(^{Dipp}NHC)_2(\mu-PAsP)$ led to the crystallization of the P_3 and PAsP radicals. Finally, we report the first reactivity results of this radical with an activated alkyne.

Results and Discussion

Synthesis of $^{Dipp}NHC=PH$ from $Na(OCP)$ (1) or $P_7(TMS)_3$ (2)

In an attempt to use $Na(OCP)$ (1) as a phosphorus transfer reagent, it was added to the imidazolium salt $[^{Dipp}NHC-H][Cl]$ (3) in THF at reflux temperatures. Upon filtration of the reaction solution and evaporation of the solvent, an off-white powder was obtained in 71% yield and identified as $^{Dipp}NHC=PH$ (4). The ^{31}P NMR spectrum shows a single phosphorus containing compound with a chemical shift of $\delta = -136.68$ ppm and a $^1J_{PH}$ coupling of 164 Hz, signifying the presence of a P-H bond. The assignment was confirmed with the report of an alternative synthesis of $^{Dipp}NHC=PH$ from phosphinidene transfer from a silylene adduct.⁵

Another route to DippNHC=PH was found in the reaction between $\text{P}_7(\text{TMS})_3$ (**2**) and the imidazolium salt **3**. The initial reaction formed the yellow salt, $[\text{DippNHC-H}][\text{P}_7(\text{TMS})_2]$, which was crystallized as the mixed salt $[\text{DippNHC-H}]_2[\text{Cl}][\text{P}_7(\text{TMS})_2]$ by adding hexane to the reaction and cooling the vessel to -35°C (see Supporting Information for a plot of the structure determined by X-ray diffraction). Resonances in the $^{31}\text{P}\{^1\text{H}\}$ NMR spectrum were consistent with previously reported $[\text{P}_7(\text{TMS})_2]^-$ anions.²⁰ The yellow, opaque solution slowly took on a dark red color, and over the course of 46 hours, the solution became dark red and homogenous.



Scheme 1. Synthetic methods to yield DippNHC=PH .

This subsequent conversion of the salt was also observed over the course of three hours in refluxing THF. DippNHC=PH was isolated from the mother liquor, which shows only the ^{31}P NMR resonance of **4**, by removal of THF under reduced pressure, followed by the extraction of the product with warm hexanes. Collection of the solid following this procedure gave an average

yield of approximately 70% based on DippNHC-HCl . In this way, DippNHC=PH is obtained as a pure powder, albeit with low atom economy.

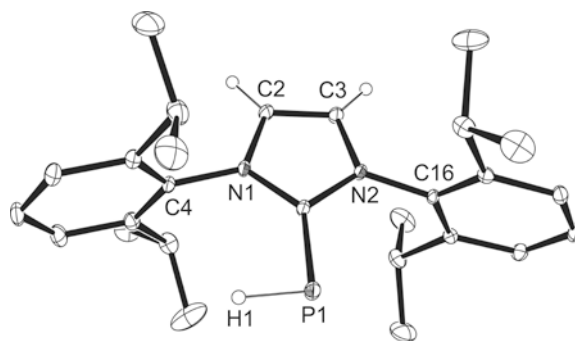


Figure 1. Solid state structure of DippNHC=PH (**4**). Hydrogen atoms save for the phosphorus and C=C bound hydrogen atoms have been omitted for clarity. Ellipsoids are shown at 30% probability.

Single crystal X-ray diffraction was used to unambiguously identify the compound (Fig. 1). Comparisons of the angles and selected distances of DippNHC=PH to Robinson's anionic $[\text{Li}][\text{DippNHC=PH}]$, the only other structurally characterized adduct, are presented in Table 1.²¹ $[\text{Li}][\text{DippNHC=PH}]$ is structurally similar to DippNHC=PH , but one of the imidazole hydrogen atoms is replaced by a solvent coordinated lithium atom. Major structural changes do not occur between the anionic and neutral parent phosphinidene complexes. A slight contraction in the bond length of C(1)-P(1) to 1.752(1) Å in the neutral compound **4** from 1.763(2) Å in $[\text{Li}][\text{DippNHC=PH}]$ is attributable to the larger electron repulsion in the anionic complex. The P(1)-H(1) bond in the neutral complex is elongated to 1.306(2) Å from 1.232(19) Å in the anionic complex indicating a more polarized bond for DippNHC=PH . The C(1)-P(1)-H(1) angle is decreased significantly in DippNHC=PH to 94.5(7)° from 102(2)° in the anionic complex.

Table 1. Comparison of selected bond lengths and angles of DippNHC=PH with $[\text{Li}][\text{DippNHC=PH}]$.²¹

Å or °	DippNHC=PH	$[\text{Li}][\text{DippNHC=PH}]$
C(1)-P(1)	1.752(1)	1.763(2)
P(1)-H(1)	1.306(2)	1.232(19)
N(1)-C(1)	1.374(1)	1.362(3)
N(2)-C(1)	1.373(1)	1.366(3)
C(2)-C(3)	1.341(2)	1.351(3)
C(1)-P(1)-H(1)	94.5(7)	102(2)

Computational studies on the reaction mechanism of Na(OCP) with $[\text{NHC-H}][\text{Cl}]$

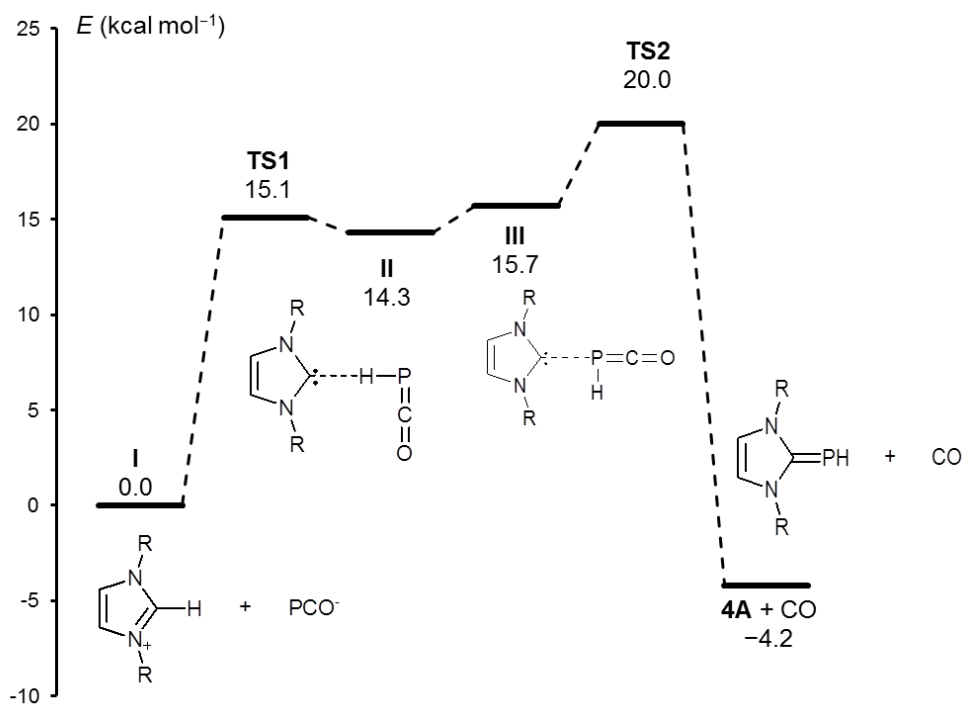
To understand the unprecedented P-atom transfer reaction of the $(\text{OCP})^-$ anion yielding the NHC=PH adduct, theoretical calculations have been performed in the gas phase on model compounds (the 2,6-di(isopropyl)phenyl substituents were replaced by methyl groups).²² All values were calculated at the B3LYP/6-31+G* level which was also employed in previous investigations in order to investigate the interaction of imidazolium cations with various anions in the gas phase.²³

Two pathways were considered leading to the carbene-phosphinidene adduct **4A**. In path (i), the phosphoethynolate anion acts as a nucleophile and attacks the C^2 carbon atom of the imidazolium cation. The formed imidazol-2-yl phosphaketene then undergoes a 1,2-H shift accompanied by the extrusion of a CO molecule. In path (ii), the $(\text{OCP})^-$ anion acts as a Brønsted base and deprotonates the C^2 atom of the imidazolium cation forming the corresponding N-heterocyclic carbene and the parent phosphaketene (H-P=C=O), which transfers its PH unit with the release of carbon monoxide. For more details see [Note1] in the ESI.

Although the phosphoethynolate anion is known to react predominantly as a P-based nucleophile with alkyl halides and compounds of the heavier group 14 elements, route (i) is quite unlikely due to the remarkable stability of the imidazolium cation. Indeed, all geometry

optimization attempts on 2,3-dihydro-1,3-dimethyl-1*H*-imidazol-2-yl phosphaketene resulted in the dissociation of the molecule into a hydrogen bonded contact ion pair.

Pathway (ii) starts with the protonation of $(\text{OCP})^-$ by the imidazolium cation forming the parent phosphaketene H-P=C=O (Scheme 2) which is significantly favored by $22.5 \text{ kcal mol}^{-1}$ over protonation of the oxygen atom. The protonation energy $\Delta E_{\text{pr}} = -330.7 \text{ kcal mol}^{-1}$ ranks the basicity of the $(\text{OCP})^-$ anion between that of chloride ($\Delta E_{\text{pr}} = -328.1 \text{ kcal mol}^{-1}$) and acetate ($\Delta E_{\text{pr}} = -349.2 \text{ kcal mol}^{-1}$).



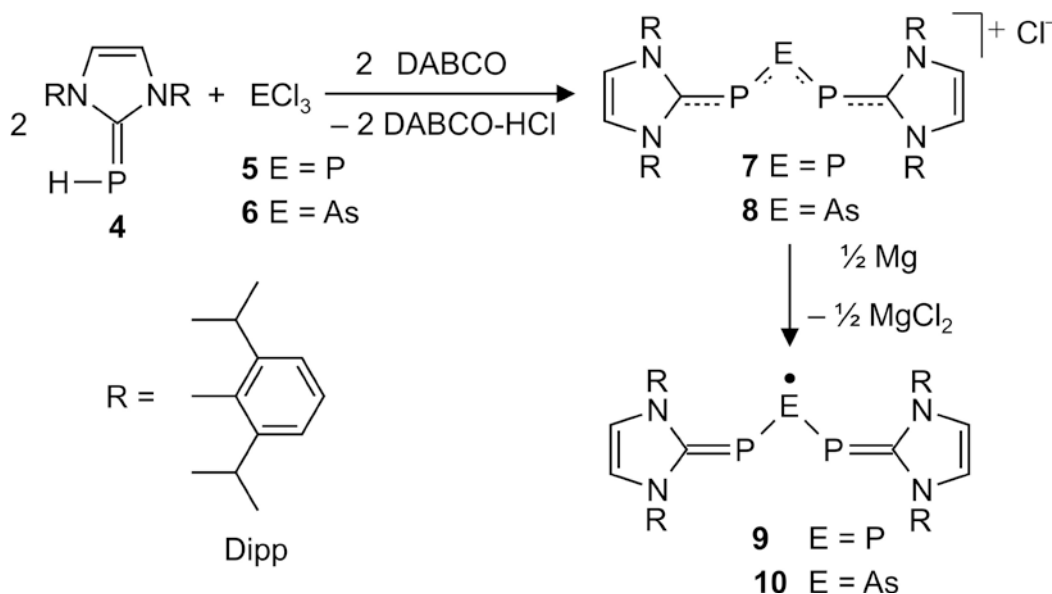
Scheme 2. Reaction pathway leading from $[\text{MeNHC-H}][\text{OCP}]$ to MeNHC=PH and CO

The minimum energy reaction pathway (MERP) is shown in Scheme 2. The hydrogen bonded complex (**II**) between the model carbene ($^{\text{Me}}\text{NHC}$) and H-P=C=O is $14.3 \text{ kcal mol}^{-1}$ less stable than the contact ion pair $[\text{MeNHC-H}][\text{OCP}]$ (**I**). The transformation from **I** to **II** is the rate determining step of the reaction with an activation barrier of $\Delta E^\ddagger = 15.1 \text{ kcal mol}^{-1}$ (compared to

I). Complex **II** can rearrange to form the slightly less stable adduct **III**, which delivers the carbene-phosphinidene adduct $^{\text{Me}}\text{NHC}=\text{PH}$ (**4A**) and carbon monoxide. The activation barrier of this final step is small ($\Delta E^\ddagger = 4.2 \text{ kcal mol}^{-1}$), and the transition state indicates the simultaneous formation of the $\text{P}-\text{C}^{\text{carbene}}$ bond and the cleavage of the $\text{P}=\text{C}(\text{O})$ bond. Compared to complex **I** the reaction energy is only slightly exothermic ($\Delta_r E = -4.3 \text{ kcal mol}^{-1}$), but after including the entropy factor (cf. formation of two species from a contact ion pair) the reaction becomes remarkably exergonic ($\Delta_r G = -14.9 \text{ kcal mol}^{-1}$).

Synthesis of P_3 and PAsP cations and radicals

The construction of the P_3 unit was achieved by the addition of half of an equivalent of PCl_3 (**5**) to a stirring THF solution of $^{\text{Dipp}}\text{NHC}=\text{PH}$ (**4**) with an equivalent of DABCO (1,4-diazabicyclo[2.2.2]octane) (Scheme 3). The solution immediately turns to emerald green from yellow, and a colorless precipitate forms. The green solution is filtered to remove DABCO-HCl and a bright green solid identified as $[(^{\text{Dipp}}\text{NHC})_2(\mu\text{-P}_3)][\text{Cl}]$ (**7**) can be isolated from the mother liquor. Likewise, upon addition of AsCl_3 (**6**) to a solution of **4** with an equivalent of DABCO, the reaction becomes dark green and a colorless precipitate forms. The green solution is filtered to remove DABCO-HCl and a green solid identified as $[(^{\text{Dipp}}\text{NHC})_2(\mu\text{-PAsP})][\text{Cl}]$ (**8**) is isolated in 55% yield as a green powder ($\lambda_{\text{max}} = 666 \text{ nm}$). A molecule, $(^{\text{Dipp}}\text{NHC}=\text{N})_2(\mu\text{-P})$, related to **7** and **8** has been synthesized from PCl_3 and 2 equivalents of $[\text{Li}][^{\text{Dipp}}\text{NHC}=\text{N}]$ by Bertrand et al.²⁴



Scheme 3. Synthesis of the cationic species $[(^{\text{Dipp}}\text{NHC})_2(\mu\text{-PEP})][\text{Cl}]$ (E = P: **7**; E = As: **8**) and the corresponding neutral radicals **9** and **10**.

The $^{31}\text{P}\{^1\text{H}\}$ NMR spectrum of $[(^{\text{Dipp}}\text{NHC})_2(\mu\text{-P}_3)][\text{Cl}]$ consists of a doublet centered at $\delta = 190.59$ ppm for the terminal P atoms and a triplet centered at $\delta = 591.88$ ppm for the central P atom both with a $^1J_{\text{PP}}$ of 505.9 Hz. This data is consistent with the analogous complex recently reported by Weigand and Frenking et al. ($\delta^{31}\text{P}$ NMR = 199.4 ppm, 597.9 ppm, $^1J_{\text{PP}} = -508.3$ Hz)¹⁸ and several other catena P_3 compounds although these are obtained as anionic compounds or metal bound species.²⁵ The green arsenic analogue $[(^{\text{Dipp}}\text{NHC})_2(\mu\text{-PAsP})][\text{Cl}]$ ($\lambda_{\text{max}} = 714$ nm) exhibited a resonance in the ^{31}P NMR spectrum at 218.92 ppm.

The facile synthesis and relative stability of $[(^{\text{Dipp}}\text{NHC})_2(\mu\text{-PEP})][\text{Cl}]$ allows for further studies into the properties of the carbene stabilized P-E-P units (E = P, As). A cyclic voltammogram (CV) was obtained of $[(^{\text{Dipp}}\text{NHC})_2(\mu\text{-P}_3)][\text{Cl}]$ and a reversible reduction wave was observed at -1.67 eV vs ferrocene/ferrocenium. The high reduction potential of the cation is attributed to the very electron rich nature of the P_3 unit due to the donating ability of the carbenes. The cations **7** and **8** were chemically reduced by stirring $[(^{\text{Dipp}}\text{NHC})_2(\mu\text{-PEP})][\text{Cl}]$ (E =

P, As) in THF with an excess of Mg^0 for one hour. The reaction solution changed color from green to dark purple. Removal of the THF and extraction of the residue into hexanes followed by cooling the hexanes solution over night at $-30\text{ }^\circ\text{C}$ yielded blue crystals of $(^{\text{Dipp}}\text{NHC})_2(\mu\text{-P}_3)$ (**9**) ($\lambda_{\text{max}} = 776\text{ nm}$). The arsenic analogue, $(^{\text{Dipp}}\text{NHC})_2(\mu\text{-PAsP})$ (**10**), was obtained as purple crystals ($\lambda_{\text{max}} = 772\text{ nm}$). The radicals have proven to be stable as a powder in an inert atmosphere for months, yet readily decompose in air.

EPR Investigations

The synthesis of phosphorus radicals has been a target for chemists because of their inherently high anisotropic ^{31}P hyperfine coupling that is well suited to the study of molecular dynamics using spin-labeling techniques and EPR spectroscopy.²⁶

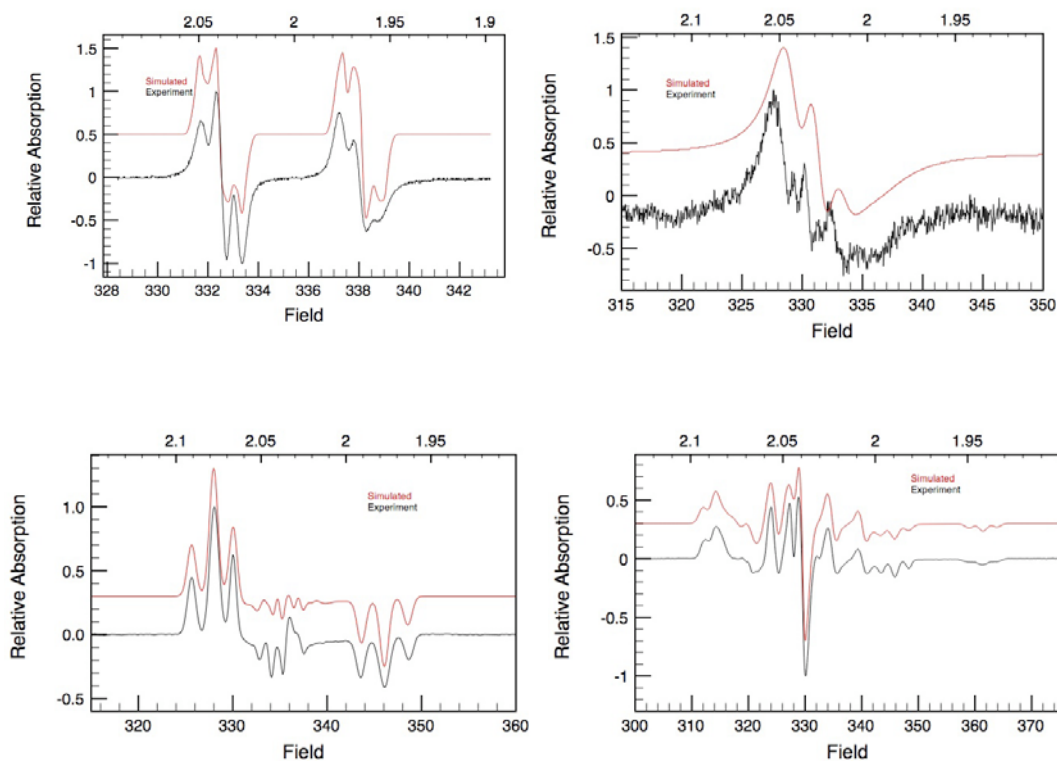


Figure 2. The experimental and simulated EPR spectra of $(^{\text{Dipp}}\text{NHC})_2(\mu\text{-P}_3)$ (top left) and $(^{\text{Dipp}}\text{NHC})_2(\mu\text{-PAsP})$ (top right) obtained at room temperature and $(^{\text{Dipp}}\text{NHC})_2(\mu\text{-P}_3)$ (bottom left) and $(^{\text{Dipp}}\text{NHC})_2(\mu\text{-PAsP})$ (bottom right) obtained at 80 K in hexane. The ESI contains further measurement and simulation information.

Two general stabilization strategies have been utilized in these syntheses. The first strategy involves steric protection of the phosphorus radical, providing kinetic stabilization. The second is to delocalize the radical into a conjugated π -system thereby inducing a thermodynamic stabilization of the phosphorus radical. The radicals synthesized herein utilize both strategies for stabilization. The combination of EPR and a single-crystal X-ray structure, shown later, confirms the nature of the $(^{\text{Dipp}}\text{NHC})_2(\mu\text{-P}_3)$ radical as having an $S = 1/2$ electron spin ground state. The EPR spectrum in solution (Figure 2, top left) was successfully simulated with an isotropic g -value of $g_{\text{iso}} = 2.010$ and a large isotropic hyperfine coupling from the central phosphorus atom (P2) of $A_{\text{iso}} = 158.6$ MHz and smaller hyperfine coupling for the two terminal phosphorus atoms, (P1) and (P3), of $A_{\text{iso}} = 10.1$ MHz. This yields an overall doublet of triplets. The spectrum line-width was modeled by unresolved hyperfine couplings from four nitrogen atoms with $A_{\text{iso}} = 4$ MHz. The frozen solution (80 K) CW (continuous wave) EPR of $(^{\text{Dipp}}\text{NHC})_2(\mu\text{-P}_3)$ (Figure 2, bottom left) exhibits a complex anisotropic coupling pattern that is well modeled with the following spin Hamiltonian parameters: $(g_{xx}, g_{yy}, g_{zz}) = (2.0112, 2.0155, 2.0043)$, P(2) $(A_{xx}, A_{yy}, A_{zz}) = (-9.3, -16.7, 505.0)$ MHz, while P(1) and P(3) exhibited $(A_{xx}, A_{yy}, A_{zz}) = (-21.1, -22.5, 74.0)$ MHz). The large disparity of the size of the isotropic ^{31}P hyperfine coupling constants indicates that a majority of the unpaired spin is localized on the central phosphorus atom, but the radical does conjugate over the other phosphorus atoms and probably slightly into the imidazole moiety as suggested by our line-width model of the solution spectrum. The large anisotropy of the (P2) hyperfine coupling in particular is consistent with a large p-type orbital contribution to the SOMO as would be expected for a conjugated π -system.

The experimental EPR data are consistent with DFT calculations on the model system. As can be expected from the LUMO of cation $[(^{\text{Me}}\text{NHC})_2(\mu\text{-P}_3)]^+$ (Figure 3a), the one-electron

reduction product is a radical with high spin density on the central P atom (see the SOMO of the radical, Figure 3b). In $(^{\text{Me}}\text{NHC})_2(\mu\text{-P}_3)$, 65.6% of the Mulliken spin density is located on the central phosphorus, and 3.3% on each of the other two (terminal) P atoms with minor contributions from the imidazole N atoms (see Figure 3c). These values are in excellent agreement with the experimentally determined values of 64.4% on the central phosphorus atom, and 3.8% on each of the two terminal P atoms.

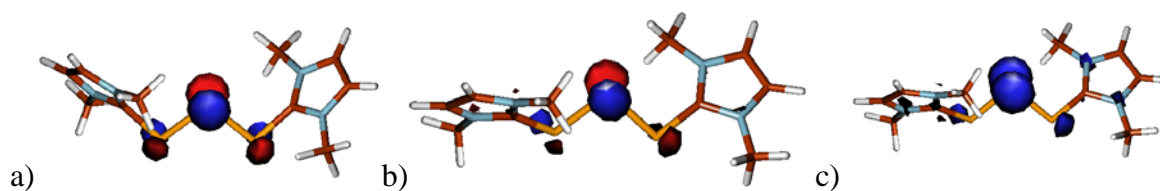


Figure 3. a) The LUMO of $[(^{\text{Me}}\text{NHC})_2(\mu\text{-P}_3)]^+$; b) SOMO of $(^{\text{Me}}\text{NHC})_2(\mu\text{-P}_3)$; c) the contour plot of the spin density (contour value: 0.005 a.u.) of $(^{\text{Me}}\text{NHC})_2(\mu\text{-P}_3)$ at the B3LYP/6-31G* level.

The room temperature solution CW EPR spectrum of $(^{\text{Dipp}}\text{NHC})_2(\mu\text{-PAsP})$ (Figure 2, top right) is very weak and rather nondescript as compared to $(^{\text{Dipp}}\text{NHC})_2(\mu\text{-P}_3)$. However, it is adequately described using a model with $g_{\text{iso}} = 2.035$, $A_{\text{iso}}(\text{As}) = 57$ MHz, and a rotational correlation time of $\tau_r = 0.13$ ns to model the spectrum asymmetry resulting from the arsenic hyperfine coupling, see below. The small splittings in the middle of the spectrum are due to two ^{31}P couplings but could not be included in a dynamics simulation (i.e. with τ_r) using EasySpin.²⁷ The frozen solution (80 K) spectrum (Figure 2, bottom right) is well defined and was successfully modeled with the following parameters for an $S = 1/2$ spin: $(g_{xx}, g_{yy}, g_{zz}) = (2.0695, 2.0326, 2.0017)$, $\text{As}(2)$: $(A_{xx}, A_{yy}, A_{zz}) = (-120.7, -141.0, 435.7)$ MHz, and $\text{P}(1), \text{P}(3)$: $(A_{xx}, A_{yy}, A_{zz}) = (-16.6, -6.3, 68.8)$ MHz. The large and anisotropic arsenic hyperfine coupling is indicative of a majority of the unpaired spin being localized on this central atom in a p-type

orbital, much as in the case of $(^{\text{Dipp}}\text{NHC})_2(\mu\text{-P}_3)$. The DFT calculations on the model $(^{\text{Me}}\text{NHC})_2(\mu\text{-PAsP})$ radical show that 67.3% of the spin density is on the arsenic and 2.0% is on each of the terminal phosphorus atoms, which is close to the experimentally determined values of 80.4% and 1.5%, respectively.

Structural Investigations

The solid-state structure of $[(^{\text{Dipp}}\text{NHC})_2(\mu\text{-P}_3)][\text{Cl}]$ (**7**) confirms the compound as a separate ion pair (Figure 4). A notable feature of **7** is the significant elongation of the carbon-phosphorous bonds from 1.752(1) Å in $^{\text{Dipp}}\text{NHC}=\text{PH}$ (**4**) to an average of 1.811(2) Å (see Table 2 for selected bond lengths of **7** – **10**). The P-P bonds, P(1)-P(2) and P(2)-P(3), are short, 2.090(1) Å and 2.097(1) Å, respectively, indicating substantial multiple bond character when compared to the standard P-P single bond length of 2.1994(3) Å in P_4 .²⁸ $[(^{\text{Dipp}}\text{NHC})_2(\mu\text{-PAsP})][\text{Cl}]$ (**8**) was also unambiguously assigned by single crystal X-ray diffraction. The carbon-phosphorous bonds are also lengthened to 1.800(2) Å while the As-P bonds are contracted to 2.202(1) Å.²⁹

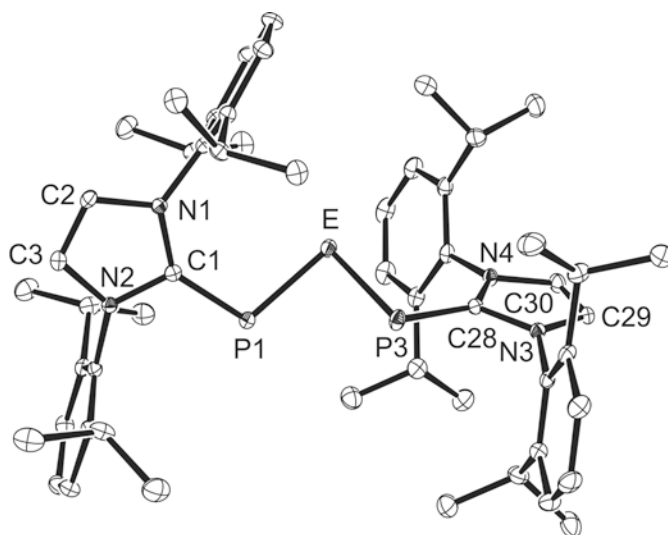


Figure 4. Representative structure plot of the solid state structures of the cations $[(^{\text{Dipp}}\text{NHC})_2(\mu\text{-PEP})][\text{Cl}]$ (E = P(2): **7**; E = As(1): **8**), the radicals $(^{\text{Dipp}}\text{NHC})_2(\mu\text{-PEP})$ (E = P2: **9**; E = As1: **10**). Solvent molecules and hydrogen atoms have been omitted for clarity. Ellipsoids are shown at 30% probability.

Table 2. Comparison of selected bond lengths and angles of $[(^{\text{Dipp}}\text{NHC})_2(\mu\text{-P}_3)][\text{Cl}]^{\text{a}}$ (**7**), $(^{\text{Dipp}}\text{NHC})_2(\mu\text{-P}_3)^{\text{a}}$ (**9**), $[(^{\text{Dipp}}\text{NHC})_2(\mu\text{-PAsP})][\text{Cl}]$ (**8**)^a, and $(^{\text{Dipp}}\text{NHC})_2(\mu\text{-PAsP})$ (**10**)^{a,b}.

Å or °	$[(^{\text{Dipp}}\text{NHC})_2(\mu\text{-P}_3)]^{\text{+}}$	$(^{\text{Dipp}}\text{NHC})_2(\mu\text{-P}_3)$	$[(^{\text{Dipp}}\text{NHC})_2(\mu\text{-PAsP})]^{\text{+}}$	$(^{\text{Dipp}}\text{NHC})_2(\mu\text{-PAsP})$
C(1)-P(1)	1.810(2)	1.763(2)	1.800(2)	1.770(3)
P(1)-E	2.090(1)	2.145(1)	2.203(1)	2.256(1)
E-P(3)	2.097(1)	2.144(1)		2.266(1)
P(3)-C(28)	1.812(2)	1.769(2)		1.763(3)
C(1)-P(1)-E	105.43(5)	105.71(6)	106.80(6)	107.31(12)
P(1)-E-P(3)	92.76(2)	90.53(3)	86.30(3)	86.53(4)
E-P(3)-C(28)	105.59(5)	105.03(6)		105.31(12)

^a Phosphorus compounds show the corresponding bonds of E replaced with P(2). Arsenic compounds show the corresponding bonds of E replaced with As(1).

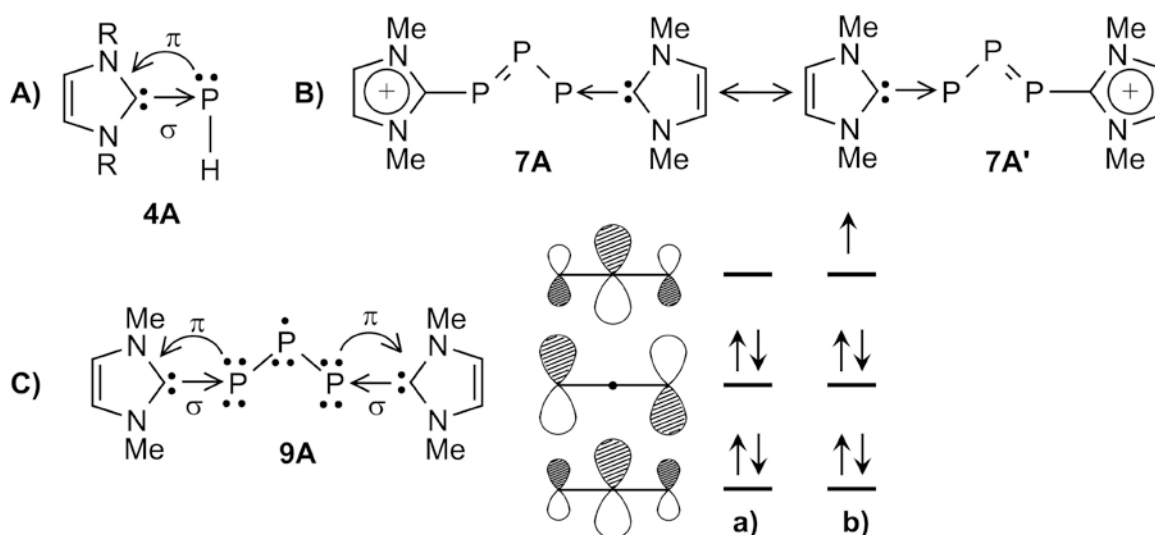
^b $(^{\text{Dipp}}\text{NHC})_2(\mu\text{-PAsP})$ contains two molecules in the unit cell. These values are for one of the molecules.

One electron reduction of the cations **7** and **8** leads to significant changes in bond lengths in the corresponding neutral radicals **9** and **10**. In $(^{\text{Dipp}}\text{NHC})_2(\mu\text{-P}_3)$ (**9**), the lengthening of P(1)-P(2) and P(2)-P(3) bonds to 2.145(1) Å and 2.144(1) Å is indicative of a weakening of the P-P interaction due to an increased electronic repulsion between the phosphorous atoms. The π^* -orbital that was empty in the cation (see Fig 3a) now contains an electron in $(^{\text{Dipp}}\text{NHC})_2(\mu\text{-P}_3)$. The contraction of the P-C bonds, P(1)-C(1) and P(3)-C(28), to 1.763(2) Å and 1.769(2) Å, respectively, occurs because the P(1) and P(3) atoms now donate more electron density into the π^* -orbital of the carbene unit.

The cation of $[(^{\text{Dipp}}\text{NHC})_2(\mu\text{-PAsP})][\text{Cl}]$ (**10**) also undergoes comparable structural changes upon one electron reduction to the neutral radical. The bonds between the arsenic and phosphorus lengthen to 2.256(1) Å and 2.266(1) Å indicating a weakening of the As-P bond. The P-C bonds in **10**, P(1)-C(1) and P(3)-C(28), contract to 1.770(3) Å and 1.763(3) Å, respectively, because of increasing donation of electron density into the π^* -orbital of the carbene moiety.

Computational Studies on the Electronic Structure of $[(^{\text{Me}}\text{NHC})_2(\mu\text{-P}_3)]^+$ and $(^{\text{Me}}\text{NHC})_2(\mu\text{-P}_3)$

Detailed studies by Frison and Sevin of the electronic structure of N-heterocyclic carbene-phosphinidene adducts like **4** indicates that the C-P bond is essentially derived by σ -donation from the carbene to the PH moiety, with a less pronounced yet substantial π -backbonding which slightly decreases the aromaticity of the five-membered C_3N_2 -ring.³⁰ Consequently, resonance structure **4A** in Scheme 4 has the largest contribution to the electronic ground state.



Scheme 4. Qualitative depiction of the resonance structures contributing largely to the electronic ground state of the A) N-heterocyclic carbene-phosphinidene adduct **4A**, B) Bis(N-heterocyclic carbene) P_3^+ cation adduct **7A, A'**, and C) Bis(N-heterocyclic carbene) P_3 radical adduct **9A**.

To gain deeper insights into the electronic structure and charge distribution of the cation and the radical, we performed molecular orbital (MO), natural bonding orbital (NBO) calculations including natural population analyses (NPA) on the geometries lying at the lowest in energy of model species $[(^{\text{Me}}\text{NHC})_2(\mu\text{-P}_3)]^+$ (**7A, A'**) and $(^{\text{Me}}\text{NHC})_2(\mu\text{-P}_3)$ (**9A**; see Scheme 4).³¹

The NPA charges are collected in Table 3 (for Mulliken charges see ESI), while Table 4 contains selected bond lengths, Wiberg bond indices, and electron density values with ellipticity at the bond critical points for the ‘computed’ cation **7A,A'** and radical **9A**. For comparison, these values were also determined for the analogous cationic and radical $[(\text{H}_2\text{C})_2(\mu\text{-P}_3)]^{+/\bullet}$ systems which contain the carbene fragment CH_2 instead of the NHC moiety.

Table 3. NPA charges (in electrons) at the B3LYP/cc-pVDZ//B3LYP/6-31+G* level of theory.

	$[(^{\text{Me}}\text{NHC})_2(\mu\text{-PP}'\text{P})]^+$	$(^{\text{Me}}\text{NHC})_2(\mu\text{-PP}'\text{P})$
P' (central)	-0.06	-0.26
P	+0.07	-0.04
$[\text{MeNHC}]$ ring	+0.45	+0.17
	$[(\text{H}_2\text{C})_2(\mu\text{-PP}'\text{P})]^+$	$(\text{H}_2\text{C})_2(\mu\text{-PP}'\text{P})$
P' (central)	+0.25	-0.06
P	+0.42	+0.33
$[\text{CH}_2]$ unit	-0.04	-0.30

Table 4. Selected bond lengths (d, Å), Wiberg bond indices (WBI, -), and electron density values (ρ , a.u.) with ellipticity (ϵ , -) at the bond critical points at the B3LYP/cc-pVDZ//B3LYP/6-31+G* level of theory. P' is the central phosphorus atom

	$[(^{\text{Me}}\text{NHC})_2(\mu\text{-PP}'\text{P})]^+$		$(^{\text{Me}}\text{NHC})_2(\mu\text{-PP}'\text{P})$	
	CP	PP'	CP	PP'
d	1.840	2.115	1.795	2.187
WBI	1.015	1.445	1.222	1.142
ρ	0.134	0.132	0.139	0.118
ϵ	0.190	0.357	0.403	0.232
	$[(\text{H}_2\text{C})_2(\mu\text{-PP}'\text{P})]^+$		$(\text{H}_2\text{C})_2(\mu\text{-PP}'\text{P})$	
	CP	PP'	CP	PP'
d	1.719	2.176	1.700	2.182
WBI	1.629	1.254	1.696	1.193
ρ	0.167	0.126	0.170	0.124
ϵ	0.211	0.103	0.268	0.129

Various electronic structures were taken into consideration to describe the electronic structure of the cation **7A** (see [Note2] in the Supporting Information for details). As the data in Table 3

show, the P₃ fragment in the cation [(^{Me}NHC)₂(μ-P₃)]⁺ is almost neutrally charged while the positive charge is equally distributed over both imidazolyl rings (+0.45 e each). The Wiberg bond index (WBI) of 1.445 and the pronounced ellipticity of the PP bonds (ε = 0.357) are consistent with substantial P-P double bond character within the P₃ unit. In contrast, the WBIs and ε at the bond critical point of the C-P bonds is rather small indicating single bond character. This leads us to propose the resonance structures **7A** and **7A'** as main contributors to the electronic ground state of the cation [(^{Me}NHC)₂(μ-P₃)]⁺ in which one imidazolyl coordinates to the P₃ unit via a σ-donor acceptor bond, while the other forms a classical C-P single bond and the P₃ units serves as a substituent to an imidazolium cation. Our analysis largely agrees with a recent energy decomposition analysis by Weigand and Frenking et al.¹⁸ It is instructive to compare the charge distribution and bonding parameters with those of the analogue (H₂C)₂(μ-PP'P): here the P atoms carry the larger part of the positive charge as expected from the electronegativity difference between carbon and phosphorus. In contrast to [(^{Me}NHC)₂(μ-P₃)]⁺ a delocalization of the double bonds is observed over the whole skeleton, showing a remarkable similarity with the pentadienyl cation. These observations underline the strong π-withdrawing effect of the imidazole rings, which are indeed accountable for the “inverted” bonding sequence with respect to the WBIs of the C-P-P'-P-C unit in [(^{Me}NHC)₂(μ-PP'P)]⁺ (1.015/1.445/1.445/1.015) compared to the parent [(H₂C)₂(μ-PP'P)]⁺ (1.629/1.254/1.254/1.629).

The parent (H₂C)₂(μ-PP'P) radical is the triphospha analogue of the pentadienyl radical containing 5 delocalized π electrons. The SOMO of this molecule (see Fig. S16 in the ESI) is centered on the central P and the C atoms with nodes at the terminal phosphorus atoms. The carbon atoms are negatively charged. On the contrary, in the “inversely polarized” radical (^{Me}NHC)₂(μ-P₃) the negative charge is mainly located on the central P atom. Upon formation of

the radical, the strength and the ellipticity of the CP bond increases (e.g. $\varepsilon = 0.403$ vs. 0.190), indicating an increase in the π -backdonation from the P lone pairs into the NHC ring. The PP bond orders and their double bond character are remarkably smaller in the radical than in the cation, although some delocalization is still observed.

The P_3 unit of the carbene supported $(^{\text{Me}}\text{NHC})_2(\mu\text{-P}_3)$ radical is valence iso-electronic with the allyl dianion radical, where the SOMO is localized mainly on the central atom (see qualitative MO diagram in Scheme 4C). We conclude that the $(^{\text{Me}}\text{NHC})_2(\mu\text{-P}_3)$ radical can be best described as a $P\text{-P}^\bullet\text{-P}$ radical coordinated by two NHC carbene units as shown in **9A** (Scheme 4) accompanied by strong backdonation from the terminal phosphorus lone pairs, which stabilizes the electron rich P_3 fragment.

Reactivity Studies

A [3+2] cycloaddition of several disubstituted acetylenes with $(^{\text{Dipp}}\text{NHC})_2(\mu\text{-P}_3)$ was attempted. Diphenylacetylene and bis(trimethylsilyl)acetylene proved to be unreactive with $(^{\text{Dipp}}\text{NHC})_2(\mu\text{-P}_3)$, yet dimethyl acetylenedicarboxylate, $(\text{MeOOC})\text{C}\equiv\text{C}(\text{COOMe})$, reacted immediately. A bright green precipitate forms upon the addition of $(\text{MeOOC})\text{C}\equiv\text{C}(\text{COOMe})$ to a hexane solution of $(^{\text{Dipp}}\text{NHC})_2(\mu\text{-P}_3)$. Analysis of the solution by $^3\text{P}\{^1\text{H}\}$ NMR spectroscopy showed resonances consistent with the $[(^{\text{Dipp}}\text{NHC})_2(\mu\text{-P}_3)]^+$ cation, a triplet centered at 588.51 ppm and a doublet centered at 189.58 ppm, both exhibiting a $^1J_{\text{PP}} = 504$ Hz, as well as a complex multiplet that was simulated as an AA'B system centered at 302.31 and 294.76 ppm. The ^1H NMR spectrum exhibited resonances consistent with both $^{\text{Dipp}}\text{NHC}$ fragments as well as methyl groups from the alkyne and yielded an integration of two imidazole moieties to one alkyne. The structure was unambiguously determined to be the 4,5-di(methylcarboxy)-1,2,3-triphospholide salt $[(^{\text{Dipp}}\text{NHC})_2(\mu\text{-P}_3)]^+[\text{P}_3\text{C}_2(\text{COOMe})_2]^-$ (**11**) utilizing single-crystal X-ray crystallography

(Figure 5). The metrical parameters of the cationic moiety of **11** correspond very well to those of $[(^{\text{Dipp}}\text{NHC})_2(\mu\text{-P}_3)][\text{Cl}]$ (**7**), indicating that there is very little cation/anion interaction (see Table 5 for selected structure parameters). The anionic moiety $[\text{P}_3\text{C}_2(\text{COOMe})_2]^-$ corresponds to similar 1,2,3-triphospholides previously reported by Goicoechea.⁷

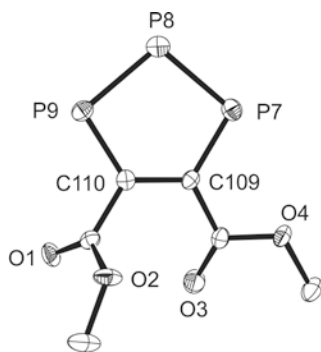
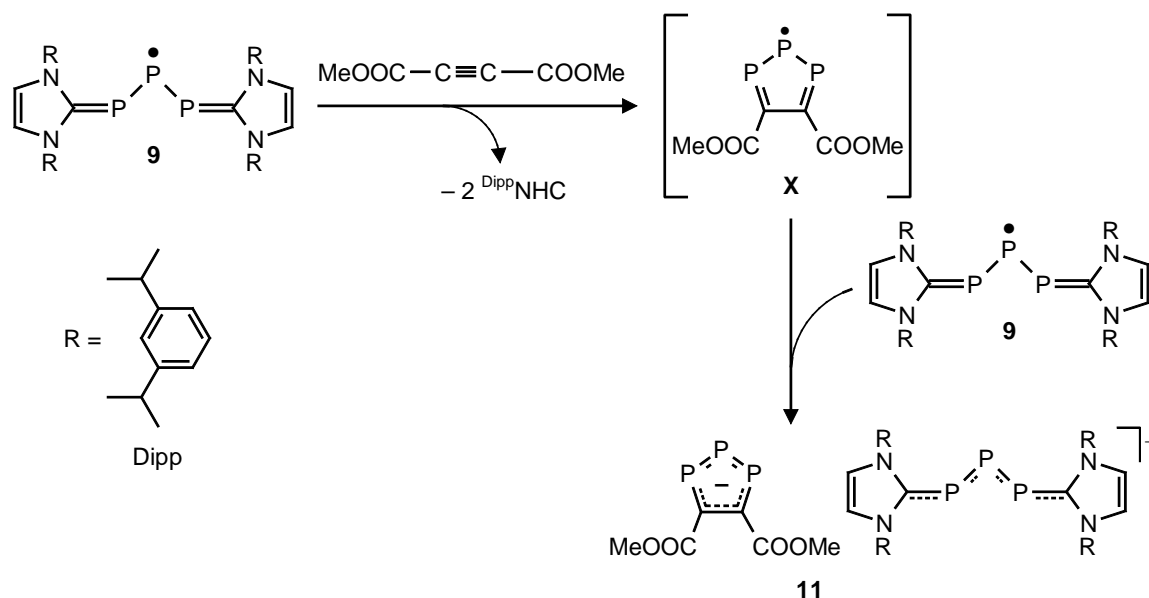


Figure 5. Solid state structure of the $[\text{P}_3\text{C}_2(\text{COOMe})_2]^-$ anion of one of two $[(^{\text{Dipp}}\text{NHC})_2(\mu\text{-P}_3)][\text{P}_3\text{C}_2(\text{COOMe})_2]$ units in the asymmetric unit of $[(^{\text{Dipp}}\text{NHC})_2(\mu\text{-P}_3)][\text{P}_3\text{C}_2(\text{COOMe})_2]$. Hydrogen atoms have been omitted for clarity. Ellipsoids are shown at 30% probability.

Table 5. Selected bond lengths and angles of $[(^{\text{Dipp}}\text{NHC})_2(\mu\text{-P}_3)][\text{P}_3(\text{CR})_2]$ (**11**).

Å or °	$[(^{\text{Dipp}}\text{NHC})_2(\mu\text{-P}_3)]^+$	Å or °	$[\text{P}_3\text{C}_2(\text{COOMe})_2]^-$
C(1)-P(1)	1.812(3)	P(7)-P(8)	2.094(1)
P(1)-P(2)	2.091(1)	P(8)-P(9)	2.098(1)
P(2)-P(3)	2.080(1)	P(7)-C(109)	1.751(3)
P(3)-C(28)	1.823(2)	P(9)-C(110)	1.753(3)
		C(109)-C(110)	1.392(3)
C(1)-P(1)-P(2)	105.01(8)	P(7)-P(8)-P(9)	100.15(4)
P(1)-P(2)-P(3)	91.43(4)	C(109)-P(7)-P(8)	98.54(9)
P(2)-P(3)-C(28)	106.60(8)	C(110)-P(9)-P(8)	98.61(9)



Scheme 5. P_3 transfer reaction from **9** to an activated alkyne to give **11**.

This transformation is a rather unique transfer of a P_3 fragment concurrent with the loss of two equivalents of free carbene. The assumed intermediate radical **X** is then thought to undergo a redox reaction with another equivalent of the P_3 radical species **9**, forming the salt pair (Scheme 5). This is a reasonable assumption due to the fact that the reduction potential of the radical is quite high and that an aromatic phospholide anion is formed in the reaction. Studies are ongoing to find reaction conditions by which a quantitative transfer of the P_3 unit from radical **9** to the acetylene is possible.

Conclusions

By utilizing a bottom-up approach, a rational route to a P_3 radical as well as a PAsP radical was achieved. Starting from a single phosphorus atom donor, in this case either $\text{Na}(\text{OCP})$ (**1**) or $\text{P}_7(\text{TMS})_3$ (**2**), the N-heterocyclic carbene adduct of the parent phosphinidene was synthesized in high yield on the gram scale. Utilizing the common pnictogen reagents PCl_3 or AsCl_3 , the cationic complexes $[(^{\text{Dipp}}\text{NHC})_2(\mu\text{-P}_3)][\text{Cl}]$ and $[(^{\text{Dipp}}\text{NHC})_2(\mu\text{-PAsP})][\text{Cl}]$ were

obtained rationally. Only with the variability offered from this bottom-up approach could the PAsP cation be synthesized, highlighting the utility of this method.

The synthesis of the radicals $(^{\text{Dipp}}\text{NHC})_2(\mu\text{-P}_3)$ and $(^{\text{Dipp}}\text{NHC})_2(\mu\text{-PAsP})$ was easily achieved with reduction by magnesium metal. The EPR studies in conjunction with the theoretical studies allow for the detailed investigation of the electronic structures of the two compounds. Both species were revealed to contain a majority spin on the central pnictogen atom, with only minor contributions from the carbenes and outside phosphorus atoms. The electronic structure of the central π -system in both $(^{\text{Dipp}}\text{NHC})_2(\mu\text{-P}_3)$ and $(^{\text{Dipp}}\text{NHC})_2(\mu\text{-PAsP})$ is thus analogous to the allyl radical dianion, which is a rare electronic structure indeed.

We are aware of the vivid discussion about the best representation of NHC carbene stabilized main group element fragment using either classical Lewis-structures or dative bonds indicated by arrows.¹⁹ Note that for **7A**, **7A'** in Scheme 4 no simple Lewis-structure can be found which is in accord with the NPA charge analysis. The classical description with two positively charged imidazolium rings requires a significantly negatively charged P_3 unit that, however, is slightly positively charged. Therefore we propose a structure that is in between the classical Lewis-structure and one with dative $\text{NHC}\rightarrow\text{P}$ bonds.

The radicals **9** and **10** are best described with two dative bonds between the NHC carbene units and central P_3 or PAsP fragment based on the NPA analyses and bond descriptors arrived from an AIM analysis. Here a classical Lewis-structure would imply positively charged imidazolium rings and a highly negatively charged (formally -2 e) main group element fragment. This is in contradiction to our findings that give less than -0.5 e on the P_3 or PAsP fragment.

Finally, a cycloaddition of the radical $(^{\text{Dipp}}\text{NHC})_2(\mu\text{-P}_3)$ (**9**) with dimethyl acetylene dicarboxylate coupled to a redox reaction was achieved yielding a salt pair **11** of the cation **7** and a 1,2,3-triphospholide. Although attempts to fully convert $[(^{\text{Dipp}}\text{NHC})_2(\mu\text{-P}_3)][\text{Cl}]$ to $[\text{P}_3(\text{CR})_2]^+$ were unsuccessful, this reaction supports the view that N-heterocyclic carbenes act as “stabilizing ligands” to reactive main group fragments such as the P_3 and PAsP radicals and allow their transfer to substrate molecules. This approach for the synthesis of main group element compounds merits further exploration.

Acknowledgement. This work was supported by the Swiss National Science Foundation (SNF), the ETH Zurich, and the Sun Yat-Sen University. Further generous support by the BASF in form of a JONAS grant to A.M.T. is acknowledged. J.H. acknowledges financial support from the ARC/FT120100421. We would like to thank Enrica Bordignon for assistance with low temperature EPR measurements and Amos J. Rosenthal for the crystal data for compound **11**.

Supporting Information Available. Experimental details can be found in the supplementary information. Crystallographic details for $^{\text{Dipp}}\text{NHC}=\text{PH}$ CCDC 937637, $[(^{\text{Dipp}}\text{NHC})_2(\mu\text{-P}_3)][\text{Cl}]$ CCDC 937642, $[(^{\text{Dipp}}\text{NHC})_2(\mu\text{-PAsP})][\text{Cl}]$ CCDC 937655, $(^{\text{Dipp}}\text{NHC})_2(\mu\text{-P}_3)$ CCDC 937654, $(^{\text{Dipp}}\text{NHC})_2(\mu\text{-PAsP})$ CCDC 937995, $[(^{\text{Dipp}}\text{NHC})_2(\mu\text{-P}_3)][\text{P}_3\text{C}_2(\text{COOMe})_2]$ CCDC 937996, and $[(^{\text{Dipp}}\text{NHC}-\text{H})_2][\text{Cl}][\text{P}_7(\text{TMS})_2]$ CCDC 937641, are available in cif format and refinement details can be found in the ESI.

References.

- ¹ (a) A. Marinetti and F. Mathey, *J. Am. Chem. Soc.*, 1982, **104**, 4484-4485; (b) M. J. v. Eis, H. Zappey, F. J. J. de Kanter, W. H. de Wolf, K. Lammertsma and F. Bickelhaupt, *J. Am. Chem. Soc.*, 2000, **122**, 3386-3390; (c) K. Lammertsma, A. W. Ehlers and M. L. McKee, *J. Am. Chem. Soc.*, 2003, **125**, 14750-14759; (d) M. L. G. Borst, R. E. Bulo, C. W. Winkel, D. J. Gibney, A. W. Ehlers, M. Schakel, M. Lutz, A. L. Spek and K. Lammertsma, *J. Am. Chem. Soc.*, 2005, **127**, 5800-5801; (e) N. H. T. Huy, S. Hao, L. Ricard and F. Matthey, *Organometallics*, 2006, **25**, 3152-3155; (f) I. Kalinina and F. Matthey, *Organometallics*, 2006, **25**, 5031-5034.
- ² (a) S. Shah and J. D. Protasiewicz, *Chem. Commun.*, 1998, **15**, 1585-1586; (b) U. J. Kilgore, H. Fan, M. Park, E. Urneezius, J. D. Protasiewicz and D. Mindiola, *Chem. Commun.*, 2009, **41**, 4521-4523.
- ³ A. Velian and C. C. Cummins, *J. Am. Chem. Soc.*, 2012, **134**, 13978-13981.
- ⁴ (a) Z. Benkő, D. Gudat and L. Nyulászi, *Chem. Eur. J.*, 2008, **14**, 902-908; (b) Z. Benkő, S. Buruch, D. Gudat, M. Nieger, L. Nyulászi and N. Shore, *Dalton Trans.*, 2008, 4937; (c) Z. Benkő, D. Gudat and L. Nyulászi, *C. R. Chimie*, 2010, **13**, 1048-1053.
- ⁵ K. Hansen, T. Szilvási, B. Blom, S. Inoue, J. Epping and M. Driess, *J. Am. Chem. Soc.*, 2013, **135**, 11795-11798.
- ⁶ C. M. Knapp, B. H. Westcott, M. A. C. Raybould, J. E. McGrady and J. M. Goicoechea, *Angew. Chem., Int. Ed.*, 2012, **51**, 9097-9100.
- ⁷ (a) R. S. P. Turbervill, A. R. Jupp, P. S. B. McCullough, D. Ergöçmen and J. M. Goicoechea, *Organometallics*, 2013, **32**, 2234-2244; (b) R. S. P. Turbervill and J. M. Goicoechea, *Inorg. Chem.*, 2013, **52**, 5527-5534.
- ⁸ (a) A. R. Jupp and J. M. Goicoechea, *Angew. Chem., Int. Ed.*, 2013, **53**, 10064-10067; for a first synthesis of Li(OCP) see: (b) G. Becker, W. Schwarz, N. Seidler and M. Westerhausen, *Z. Anorg. Allg. Chem.* **1992**, 612, 72; (c) G. Becker, G. Heckmann, K. Hübler and W. Schwarz, *Z. Anorg. Allg. Chem.* **1995**, 621, 34
- ⁹ I. Krummenacher and C. C. Cummins, *Polyhedron*, 2012, **32**, 10-13.
- ¹⁰ (a) F. F. Puschmann, D. Stein, D. Heift, C. Hendrikson, Z. A. Gal, H.-F. Grützmacher and H. Grützmacher, *Angew. Chem., Int. Ed.*, 2011, **50**, 8420-8423; (b) D. Heift, Z. Benkő and H. Grützmacher, *Dalt. Trans.* 2014, **43**, 831-840.
- ¹¹ (a) D. Martin, M. Soleilhavoup and G. Bertrand, *Chem. Sci.*, 2011, **2**, 389-399; (b) C. D. Martin, M. Soleilhavoup and G. Bertrand, *Chem. Sci.*, 2013, **4**, 3020-3030.
- ¹² M. Y. Mariham, Y. Wang, Y. Xie, P. Wei, H. F. Schaefer, P. v. R. Schleyer and G. H. Robinson, *Science*, 2008, **321**, 1069-1071.
- ¹³ A. Sidiropoulos, C. Jones, A. Stasch, S. Klein and G. Frenking, *Angew. Chem., Int. Ed.*, 2009, **48**, 9701-9704.
- ¹⁴ C. Jones, A. Sidiropoulos, N. Holzmann, G. Frenking and A. Stasch, *Chem. Commun.*, 2012, **48**, 9855-9857.
- ¹⁵ H. Braunschweig, R. D. Dewhurst, K. Hammond, J. Mies, K. Radacki and A. Vargas, *Science*, 2012, **33**, 1420-1422.
- ¹⁶ (a) O. Back, G. Kuchenbeiser, B. Donnadiou and G. Bertrand, *Angew. Chem., Int. Ed.*, 2009, **48**, 5530-5533; (b) J. D. Masuda, W. W. Schoeller, B. Donnadiou and G. Bertrand,

Angew. Chem. Int. Ed., 2007, **46**, 7052-7055; (c) C. D. Martin, C. M. Weinstein, C. E. Moore, A. L. Rheingold and G. Bertrand, *Chem. Commun.*, 2013, **49**, 4486-4488.

¹⁷ Y. Wang, Y. Xie, P. Wei, R. B. King, H. F. Schaefer III, P. v. R. Schleyer and G. H. Robinson, *J. Am. Chem. Soc.*, 2008, **130**, 14970-14971.

¹⁸ M. H. Holthausen, S. K. Surmiak, P. Jerabek, G. Frenking and J. J. Weigand, *Angew. Chem., Int. Ed.*, 2013, **52**, 11078-11082.

¹⁹ D. Himmel, I. Krossing and A. Schnepf, *Angew. Chem. Int. Ed.*, 2013, DOI: 10.1002/anie.201300461.

²⁰ V. G. Fritz, J. Härer and E. Matern, *Z. Anorg. Allg. Chem.*, 1983, **504**, 38-46.

²¹ Y. Wang, Y. Xie, M. Y. Abraham, R. J. Gilliard Jr., P. Wei, H. F. Schaefer, III, P. V. R. Schleyer and G. H. Robinson, *Organometallics*, 2010, **29**, 4778-4780.

²² M. J. Frisch, H. B. Schlegel, G. E. Scuseria, M. A. Robb, J. R. Cheeseman, G. Scalmani, V. Barone, B. Mennucci, G. A. Petersson, H. Nakatsuji, M. Caricato, X. Li, H. P. Hratchian, A. F. Izmaylov, J. Bloino, G. Zheng, J. L. Sonnenberg, M. Hada, M. Ehara, K. Toyota, R. Fukuda, J. Hasegawa, M. Ishida, T. Nakajima, Y. Honda, O. Kitao, H. Nakai, T. Vreven, J. A. Montgomery, Jr., J. E. Peralta, F. Ogliaro, M. Bearpark, J. J. Heyd, E. Brothers, K. N. Kudin, V. N. Staroverov, R. Kobayashi, J. Normand, K. Raghavachari, A. Rendell, J. C. Burant, S. S. Iyengar, J. Tomasi, M. Cossi, N. Rega, J. M. Millam, M. Klene, J. E. Knox, J. B. Cross, V. Bakken, C. Adamo, J. Jaramillo, R. Gomperts, R. E. Stratmann, O. Yazyev, A. J. Austin, R. Cammi, C. Pomelli, J. W. Ochterski, R. L. Martin, K. Morokuma, V. G. Zakrzewski, G. A. Voth, P. Salvador, J. J. Dannenberg, S. Dapprich, A. D. Daniels, Ö. Farkas, J. B. Foresman, J. V. Ortiz, J. Cioslowski and D. J. Fox, Gaussian., *Gaussian, Inc.*, Wallingford CT, 2009.

²³ O. Hollóczki, D. Gerhard, K. Massone, L. Szarvas, B. Németh, T. Veszprémi and L. Nyulászi, *New J. Chem.*, 2010, **34**, 3004-3009.

²⁴ O. Back, B. Donnadieu, M. v. Hopffgarten, S. Klein, R. Tonner, G. Frenking and G. Bertrand, *Chem. Sci.*, 2011, **2**, 858-861.

²⁵ (a) Jutzi et al. reported the synthesis of a [R-P₃-R] (R = 2,4,6-tri-*tert*-butylphenyl) moiety that exhibits ³¹P resonances in the *trans/trans* species centered at 494.1(d) and 295.5(t) ppm with a 430.1 Hz coupling. The *cis/trans* species has three ³¹P NMR resonances: one for the central phosphorus atom centered at 443 ppm (dd, ¹J_{PP} = 575 Hz, 590 Hz), and ones at 225 ppm (dd, ¹J_{PP} = 575 Hz, ²J_{PP} = 94 Hz) and 134 ppm (dd, ¹J_{PP} = 590 Hz, ²J_{PP} = 94 Hz) for the two terminal phosphorus atoms: P. Jutzi, N. Brusdeilins, U. Meyer and S. Opiela, *Phosphorus, Sulfur, Silicon and the Related Elements*, 2006, **76**, 53-56; (b) Niecke also reported an anionic P₃ complex, [Li][(TMS)₂CP₃C(TMS)₂], that exhibits resonances centered at 548 ppm (d) and 208 ppm (t) with a 524 Hz coupling: V. Thelen, D. Schmidt, M. Nieger, E. Niecke and W. E. Schoeller, *Angew. Chem.*, 1996, **108**, 354-356.

²⁶ (a) Spin Labeling, Theory and Applications (Ed.: L. J. Berliner), Academic Press, New York 1976; (b) Atomic anisotropic coupling constants obtained from Hartree-Fock calculations: J. R. Morton and K. F. Preston, *J. Magn. Reson.*, 1978, **30**, 577-582; (c) A. Armstrong, T. Chivers and R. T. Boere, *ACS Symp. Ser.*, 2005, **917**, 66-80; (d) S. Marque and P. Tordo, *Top. Curr. Chem.*, 2005, **250**, 43-76; (e) P. P. Power, *Chem. Rev.* 2003, **103**, 789-810; (f) M. Geoffroy, *Recent Res. Dev. Phys. Chem.*, 1998, **2**, 311-321.

- ²⁷ S. Stoll and A. Schweiger, EasySpin, a comprehensive software package for spectral simulation and analysis in EPR. *J. Magn. Res.*, 2006, **178**, 42-55.
- ²⁸ B. M. Cossairt, C. C. Cummins, A. R. Head, D. L. Lichtenberger, R. J. F. Berger, S. A. Hayes, N. W. Mitzel and G. Wu, *J. Am. Chem. Soc.*, 2010, **132**, 8459-8465.
- ²⁹ This distance was compared to the known anionic PAsP molecules. Niecke et al. describes the synthesis and characterization of [Li][(TMS)₂CPAsPC(TMS)₂] which is reported to contain P(1)-As(1) bond length of 2.2546(13) Å and a ³¹P shift of 529.2 ppm, highlighting the difference in charge at the phosphorus atom: A. B. Rozhenko, A. Ruban, V. Thelen, M. Nieger, K. Airola, W. W. Schoeller and E. Niecke, *Eur. J. Inorg. Chem.*, 2012, **15**, 2502-2507.
- ³⁰ (a) G. Frison and A. Sevin, *J. Phys. Chem. A*, 1999, **103**, 10998-11003; (b) G. Frison and A. Sevin, *J. Organomet. Chem.*, 2002, **643**, 105-111.
- ³¹ E. D. Glendening, A. E. Reed, J. E. Carpenter, J. A. Bohmann, C. M. Morales and F. Weinhold, *NBO 5.0.*, Theoretical Chemistry Institute, University of Wisconsin, Madison, 2001.